We are IntechOpen, the world's leading publisher of Open Access books
Built by scientists, for scientists

6,900
Open access books available

185,000
International authors and editors

200M
Downloads

154
Countries delivered to

Our authors are among the

TOP 1%
most cited scientists

12.2%
Contributors from top 500 universities

CLARIVATE ANALYTICS

BOOK CITATION INDEX

INDEXED

WEB OF SCIENCE™

Selection of our books indexed in the Book Citation Index
in Web of Science™ Core Collection (BKCI)

Interested in publishing with us?
Contact book.department@intechopen.com

Numbers displayed above are based on latest data collected.
For more information visit www.intechopen.com

Assessment of a Parametric Hurricane Surface Wind Model for Tropical Cyclones in the Gulf of Mexico

Kelin Hu, Qin Chen and Patrick Fitzpatrick

Additional information is available at the end of the chapter

1. Introduction

Tropical cyclones, which generate storm surges, wind waves, and flooding at landfall, are a major threat to human life and property in coastal regions throughout the world. The United States, the northern Gulf of Mexico, and in particular the Louisiana Gulf coast, are very susceptible to the impacts of frequent tropical storms and hurricanes due to its tropical/subtropical location and unique bathymetric, geometric, and landscape features. Severe coastal flooding, enormous property damage, and loss of life are ubiquitously associated with tropical cyclone landfalls, and this devastation was no more evident than during Hurricanes Katrina and Rita in 2005, and Gustav and Ike in 2008. Over 1800 people lost their lives and several major coastal populations were crippled for months after the hurricanes passed. It is critically important to make timely and accurate forecasts of hurricane winds, surge, and waves. The prediction of hurricane surface winds is of specific importance because it directly forces storm surge and wave models, and controls their forecast accuracy.

In the past several decades, numerous wind models and products have been developed to hindcast and forecast hurricane surface wind fields. Methodologies include H*Wind kinematic analysis winds [1], steady-state slab planetary boundary (PBL) models [2-3], interactive objective kinematic analysis system which combine steady-state slab PBL models with observations such as IOKA [4], and weather model output (operational models as well as mesoscale research models such as the Weather Research and Forecasting Model, known as WRF). After landfall, an exponentially based filling model for central pressure is sometimes applied to the PBL schemes [5].

However, many applications utilize analytical parametric formulations which represent radial profiles of tropical cyclone winds. The schemes are "parametric" in that the radial wind variation depends on just a few parameters, such as the maximum winds, the radius of max-

INTECH
open science | open minds

imum wind, and central pressure. The relative simplicity, near-zero computational cost, and flexible grid resolution favors the use of parametric winds for: assessing hurricane wind return periods and risk modeling for insurance underwriting; engineering applications; hindcasting tropical cyclone studies; and forcing of wave and surge models [6-7]. The equations exploit the basic structure of tropical cyclones in which pressure decreases exponentially towards the center then levels off in the eye, while the winds increase exponentially toward the center, then decrease to calm inside the eyewall. Radial wind profiles have evolved from the Rankine combined vortex formulation (where solid-body rotation is assumed inside the eyewall, then tangential winds decrease by a radial scaling parameter) to one in which a rectangular hyperbola approximation to radial pressure variation is used [8]. This basic concept has resulted in many wind profile relationships (e.g., [9-10]).

However, the most popular scheme is based on the 1980 Holland wind profile [11]. Since tropical cyclone winds contain significant radial profile variations, Holland modified the Schloemer equation [8] to represent a spectrum of pressure-varying rectangular hyperbolas:

$$p(r) = p_c + (p_n - p_c)e^{-\left(\frac{R_m}{r}\right)^B}$$

(1)

which includes an additional scaling parameter B:

$$B = \frac{V_m^2 \rho_a e}{p_n - p_c}$$

(2)

and a wind profile given by:

$$V(r) = \left[\frac{B}{\rho_a}\left(\frac{R_m}{r}\right)^B (p_n - p_c)e^{-(R_m/r)^B} + \gamma\left(\frac{rf}{2}\right)^2\right]^x - \gamma\left(\frac{rf}{2}\right)$$

(3)

where p is the pressure at radius r, p_c is the central pressure, p_n is the ambient pressure, R_m is the radius of maximum wind V_m, V is the wind at r, ρ_a is the air density, f is the Coriolis parameter ($f = 2\Omega \sin\phi$), Ω is the rotational frequency of the earth, ϕ is the latitude, and e is the base of the natural logarithm. B is the wind shape parameter with values typically between 1 and 2.5; for a given intensity, larger B values concentrate more of the pressure drop near R_m and the wind profile becomes more "peaked." Holland [11] assumed cyclostrophic balance where $x = 0.5$ and $\gamma = 0$. However, Hu et al. [12] retained the Coriolis terms ($\gamma = 1$) and showed that excluding the Coriolis effect in the parameter B, that is, using Eq. (2) instead of Eq. (4) to determine B, can lead to 20% errors of V_m for weak but large tropical cyclones, defaulting to gradient wind balance ($V_g = V$).

While popular, the Holland formulation [11] is known to have problems. It cannot represent double eyewalls. Another issue is the inability to accurately represent the eyewall and outer-core winds simultaneously; it can match the outer wind profile accurately but fails to capture the rapid decrease of wind just outside the eyewall (and often underestimates the true V_m), and

conversely may represent the eyewall winds well but decrease too rapidly far away from the center [13]. Willoughby et al. [14] proposed an alternative piecewise continuous wind profiles, while others have suggested alternate expressions for B [15-17]. Recently, Holland et al. [6] proposed a cyclostrophic expression ($\gamma = 0$) in which x varies linearly with radius outside the eyewall, and can also be tuned to match observations or bimodal wind profiles.

However, the biggest deficiency with [11] is the 2D nature of the equation, implying that the vortex is symmetric. Actual tropical cyclone wind fields are rarely symmetric, especially for landfalling situations. Xie et al. [18] improved the Holland model by considering asymmetry. Mattocks and Forbes [19] developed an asymmetric wind model based on Xie et al.'s approach [18] and employed it in the storm surge model ADCIRC. In their models, R_m is replaced by a directionally varying $R_m(h)$, where h is the azimuthal angle around the center of the storm. The National Hurricane Center (NHC) forecast advisories and the Automated Tropical Cyclone Forecasting (ATCF) product provide hurricane track and surface (i.e., 10 m) wind forecasts, in which the storm structure is depicted by the radii of specified wind speeds (34, 50, 64, and 100 knots) in four quadrants. The four-quadrant information is used to compute $R_m(h)$ at any azimuth through a fitting procedure. Notice that the gradient wind expression ($x = 0.5$; $\gamma = 1$) in Eq. (3) excludes the translational velocity generated by the moving hurricane. This is inconsistent with the NHC forecast wind data that include both the vortex-related and translational wind speeds. Therefore, the translational portion of the wind speed will have to be removed from the forecast (or observed values) before applying Eq. (3). Moreover, normally for each quadrant, only the largest available specified wind velocity and its radius are used in existing asymmetric parametric wind models. Owing to the complexity of actual hurricanes, it is important and necessary to make full use of all available forecast wind data to improve the accuracy of a parametric hurricane wind model.

A method to blend the Holland scheme [11] with asymmetries was developed by [12], and is described in the next section. This paper assesses Hu et al.'s [12] parametric hurricane surface wind model using field observations of several historical tropical cyclones in the Gulf of Mexico. In-situ measurements of wind speed and wind direction at 12 offshore buoys in the Gulf of Mexico and the hurricane wind hindcasts from the NHC are utilized as the reference to evaluate the predictive skills of the parametric model. Both major hurricanes and large tropical storms are selected. The resultant hurricane wind fields are merged with the available background wind fields to cover the entire Gulf of Mexico and part of the Atlantic basin, which are used to drive basin-scale storm surge and wind wave models. Statistical tools are used to quantify the accuracy of the hindcasted wind fields. A fully coupled storm surge and wind wave modeling system is then employed to demonstrate the importance of the accuracy of the parametric wind model for surge and wave hindcasts/forecasts in comparison with field observations.

2. Model description

Hu et al. [12] improved a parametric hurricane wind model based on the asymmetric Holland-type vortex models. The model creates a two-dimensional surface wind field based on the

NHC forecast (or observed) hurricane wind and track data. Three improvements have been made to retain consistency between the input parameters and the model output and to better resolve the asymmetric structure of the hurricane. Please refer to [12] for details.

First, in determination of the shape parameter B, the Coriolis effect is included, and the range restriction suggested by Holland [11] of 1.0-2.5 is removed. The parameter B is expressed as follows,

$$B = \frac{\left(V_{gm}^2 + V_{gm} R_m f\right)\rho_a e}{p_n - p_c} \tag{4}$$

If the Coriolis effect is neglected ($f = 0$), Eq. (4) returns to Eq. (2), the commonly used form of the parameter B.

Second, the effect of the translational velocity of a hurricane is excluded from the input of specified wind speeds before applying the Holland-type vortex to avoid exaggeration of the wind asymmetry. The translational velocity is added back in at the very end of the procedure.

Third, a new method has been introduced to develop a weighted composite wind field that makes full use of all wind parameters, not just the largest available specified wind speed and its 4-quadrant radii. For each set of specified wind speeds (30, 50 or 64 knots) and their radii, a gradient wind field can be calculated. Obviously, near the radii of one specified wind speed in four quadrants, the wind field based on the same specified wind speed would be much more accurate than other wind fields and should be assigned the most weight in the combined wind field, while simultaneously, the weighting coefficient for other wind fields should approach zero.

3. Recent tropical cyclone cases in the Gulf of Mexico

Ten historical tropical cyclone cases were carried out to test the performance of this wind model. They are Hurricanes Isidore and Lili in 2002, Hurricane Ivan in 2004, Hurricanes Dennis, Emily, Katrina, Rita and Wilma in 2005, and Hurricanes Gustav and Ike in 2008. The hurricane tracks and observation buoys are shown in Figure 1 [20]. The background wind is taken from the 6-hourly NCEP/NCAR Reanalysis data. For 2002 hurricanes, only the 34-knot radii at four quadrants were provided in their best track data (50- and 64-knot radii were unavailable). Due to a lack of other radii information, the wind model was not able to do the weighted composition for Hurricanes Isidore and Lili before merging with the background winds. After a brief introduction of each tropical cyclone case, comparisons of modeled and measured wind speeds/wind directions at available buoys, as well as scatter plots, are provided. Two sets of correlation coefficient (r^2) and root mean square error (RMSE), one for all data and one for observed winds stronger than 10 ms^{-1}, quantify the model performance. The latter set focuses mostly on inner-core winds.
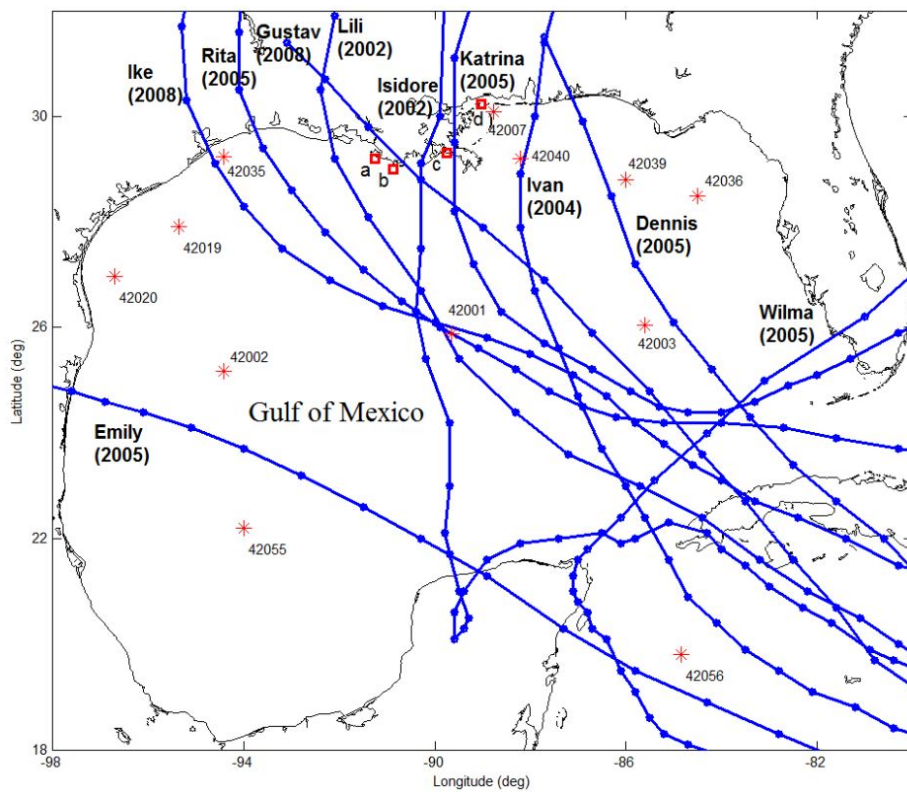
Figure 1. Tracks of ten Gulf of Mexico tropical cyclones, and buoy stations (red stars), and coastal gages (red squares, deployed for Hurricane Gustav) used for validation.

3.1. Hurricane Isidore (2002)

On September 9, a tropical wave moved off the African coast. It intensified to a hurricane late on September 19 while south of Cuba. After making landfall on Cabo Frances late on September 20, the hurricane crossed the island, then slowed as it moved westward across the Gulf of Mexico. Isidore made landfall at Telchac Puerto in Yucatán as a major hurricane on September 22. It weakened rapidly as it nearly stalled over Yucatán for 30 hours, and was only a minimal tropical storm. It then moved north and hit Grand Isle, Louisiana on September 26 as a 57-knot tropical storm, and weakened quickly into a tropical depression after moving inland. Refer to NHC's report on Isidore [21] for details.

Comparisons of modeled and measured wind speeds/wind directions at ten buoys are shown in Figure 2. The results for wind direction were quite good at all buoys. As for wind speeds, at Buoy 42001 which was very close to the hurricane track, there was an unrealistic peak around September 26, and there were some underestimations at Buoy 42007. Those discrepancies at both buoys might be caused by missing radii data. At other buoys which were relatively far from the track, such as Buoys 42036, 42039 and 42040, modeled wind speeds compared very well with the measurements. Buoys 42001, 42002, 42007, 42039 and 42040 were included in scatter plots. Although the results for wind direction were good, wind speeds scattered a lot (black and blue points), especially for observed winds larger than 20 knots (10 ms^{-1}; see blue points).
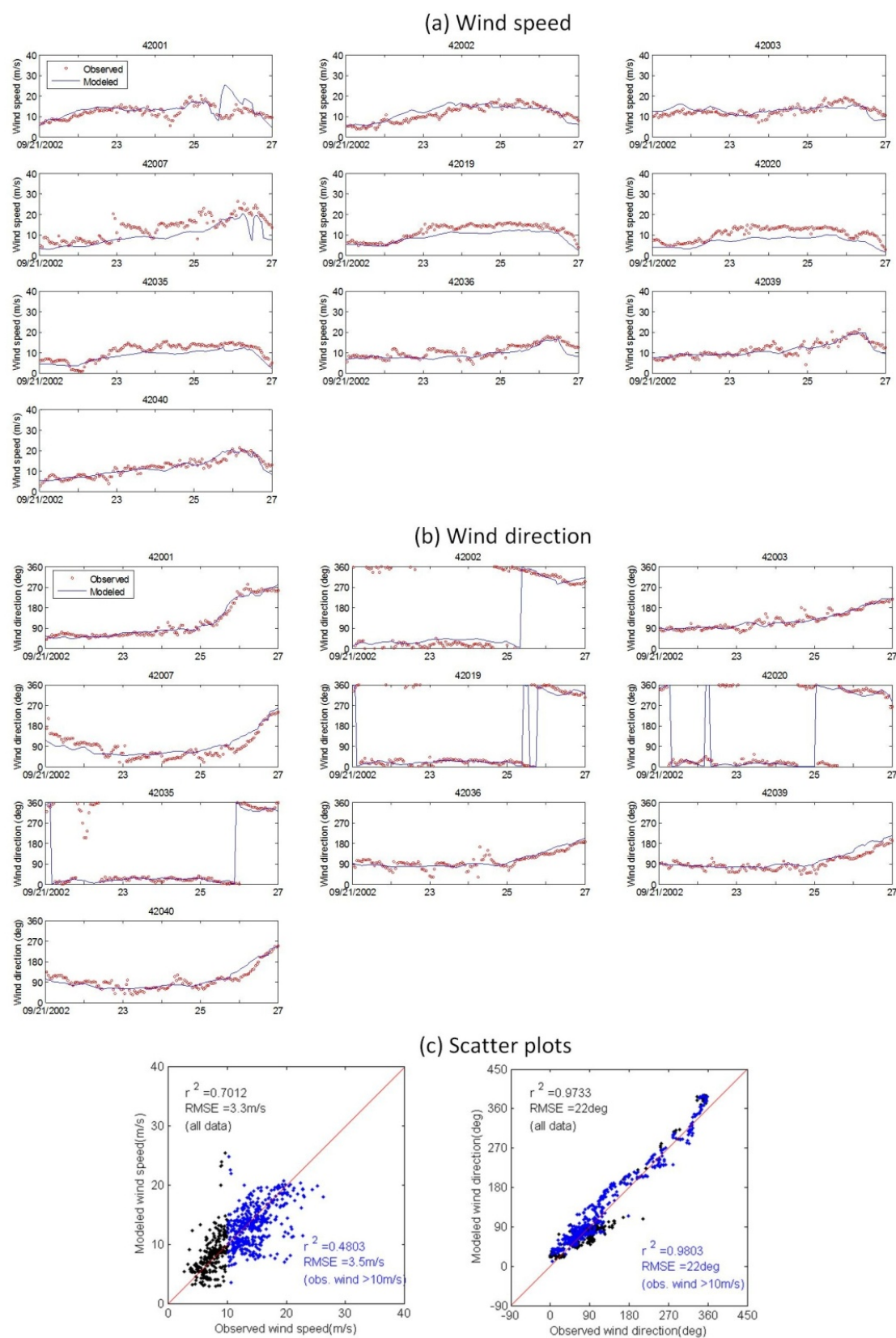
(a) Wind speed

(b) Wind direction

(c) Scatter plots

Figure 2. Wind comparisons at buoys in the Gulf of Mexico during Hurricane Isidore.

3.2. Hurricane Lili (2002)

Lili originated from a tropical wave that moved off the west coast of Africa on September 16. Lili became a hurricane on the 30th.
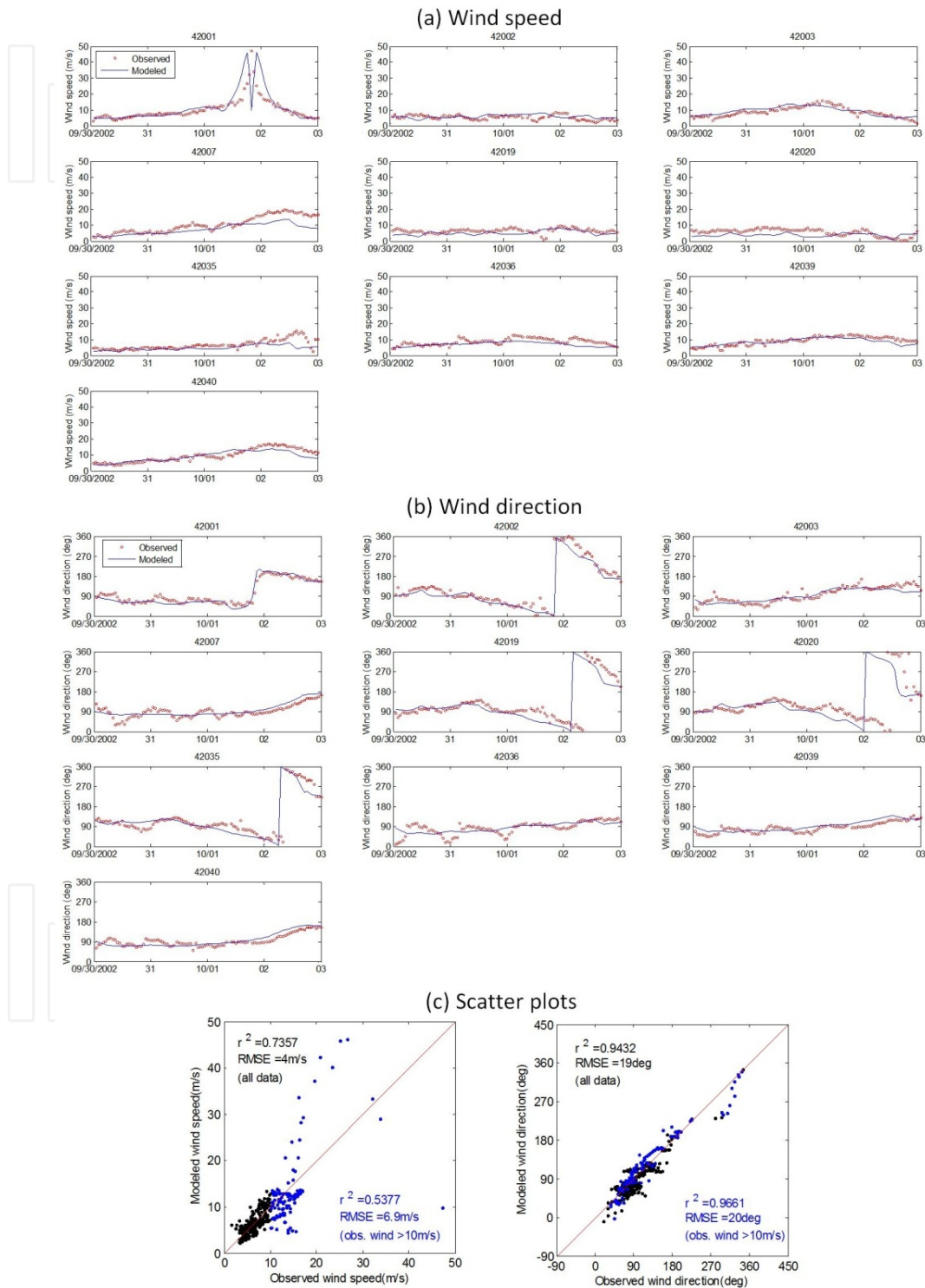

Figure 3. Wind comparisons at buoys in the Gulf of Mexico during Hurricane Lili.
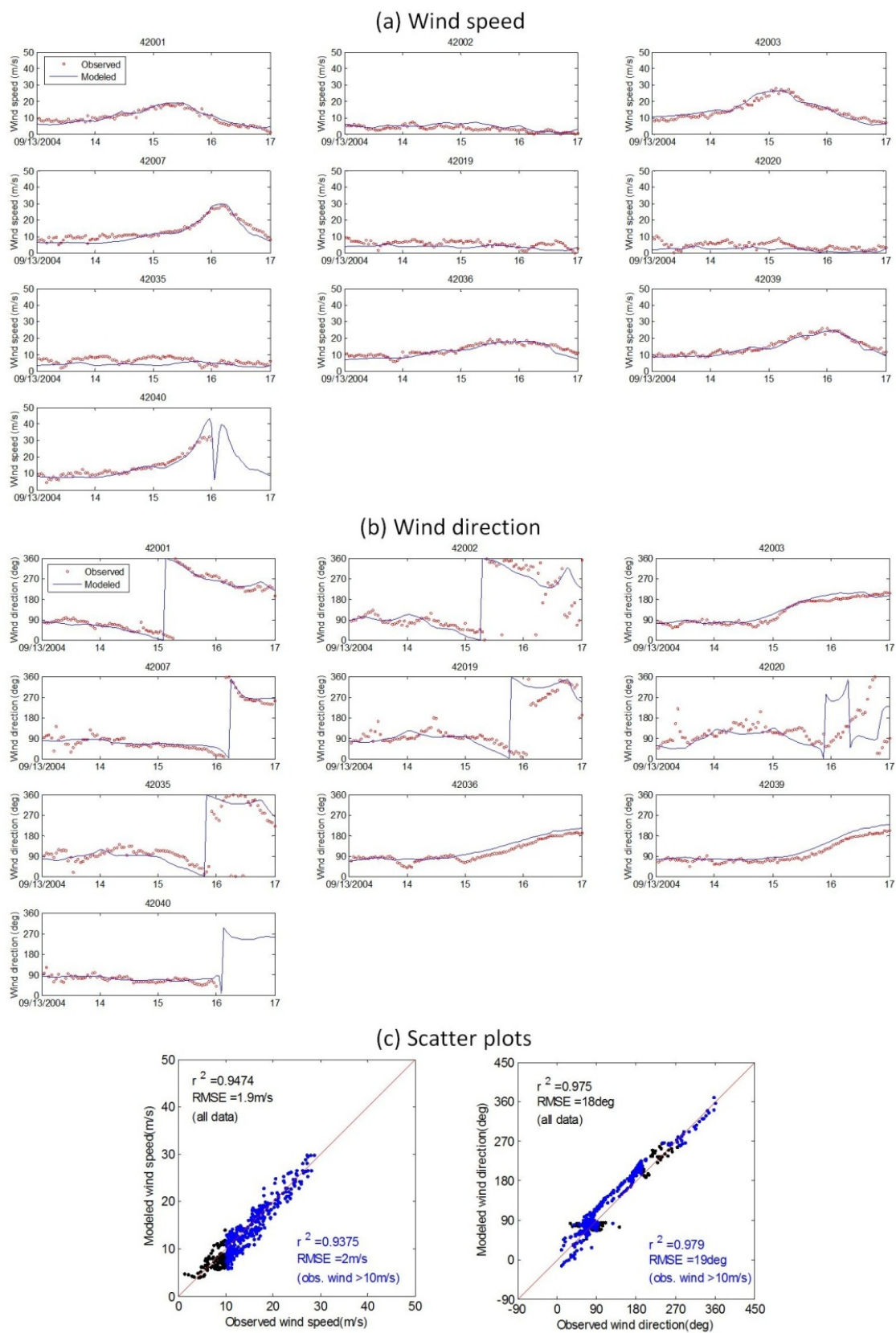
Figure 4. Wind comparisons at buoys in the Gulf of Mexico during Hurricane Ivan.

The center of the hurricane moved over the southwest tip of the Isle of Youth on the morning of October 1st. Lily turned northward and made landfall on the Louisiana coast on the 3rd, with an estimated 80-knot maximum wind speed. However, between Cuba and Louisiana, Lili intensified to 125 knots early on the 3rd over the north-central Gulf of Mexico and then rapidly weakened to 80 knots during the 13 hours until landfall. Lili was absorbed by an extratropical low on the 4th near the Tennessee/Arkansas border. Refer to NHC's report on Lili [22] for details.

Comparisons and scatter plots are shown in Figure 3. Buoys 42001, 42003, 42035 and 42040 were included in scatter plots. The results for wind direction were reasonable, while the modeled wind speeds were underestimated at Buoys 42007, 42035 and 42040. At Buoy 42001 where the hurricane almost moved through, the results showed an overestimation of wind speed. The lack of radii information and storm position error are possible explanations for the wind errors. The winds near the hurricane center change dramatically. The 6-hourly best track data cannot provide enough resolution for locations so close to the center. Scatter plots showed similar results with Isidore case.

3.3. Hurricane Ivan (2004)

Ivan was the most severe hurricane to strike the Alabama and western Florida coastlines in several decades. Ivan started as a tropical wave off the west coast of Africa on August 31, 2004. It developed into a tropical depression on September 2, 2004, in the Atlantic Ocean and strengthened into a Category 1 hurricane on the Saffir-Simpson scale 3 days later. On September 14, Ivan entered the Gulf of Mexico as a Category 5 hurricane with wind speeds of 140 knots. Ivan weakened as it moved toward the northern Gulf of Mexico and made landfall on September 16, at approximately 0650 UTC near Gulf Shores, Alabama, as a Category 3 hurricane with maximum sustained wind speeds of 113 knots. Refer to NHC's report on Ivan [23] for details.

Comparisons and scatter plots are shown in Figure 4. The results by wind model were quite good except for some overestimation of wind speed at Buoy 42040 and minor phase difference for wind direction at Buoys 42036 and 42039. Due to a malfunction at Buoy 42040 during Ivan, the recorded data for the last few hours may not be reliable. Buoys 42001, 42003, 42007, 42036 and 42039 were included in scatter plots. The RMSE values for wind speeds and wind directions are only about 2 ms^{-1} and 20 degrees.

3.4. Hurricane Dennis (2005)

Dennis was an unusually strong July major hurricane that left a trail of destruction from the Caribbean Sea to the northern coast of the Gulf of Mexico. Dennis formed from a tropical wave that moved westward from the coast of Africa on June 29. Dennis traversed a long section of western Cuba before emerging into the Gulf of Mexico on July 9. Dennis gradually intensified over the Gulf of Mexico, then rapidly intensified on July 9-10. Maximum sustained winds reached a peak of 125 knots on July 10. Thereafter, the maximum sustained winds decreased to 105 knots and the central pressure rose to 946 mb before Dennis made

landfall on Santa Rosa Island, Florida, between Navarre Beach and Gulf Breeze the same day. Refer to NHC's report on Dennis [24] for details.
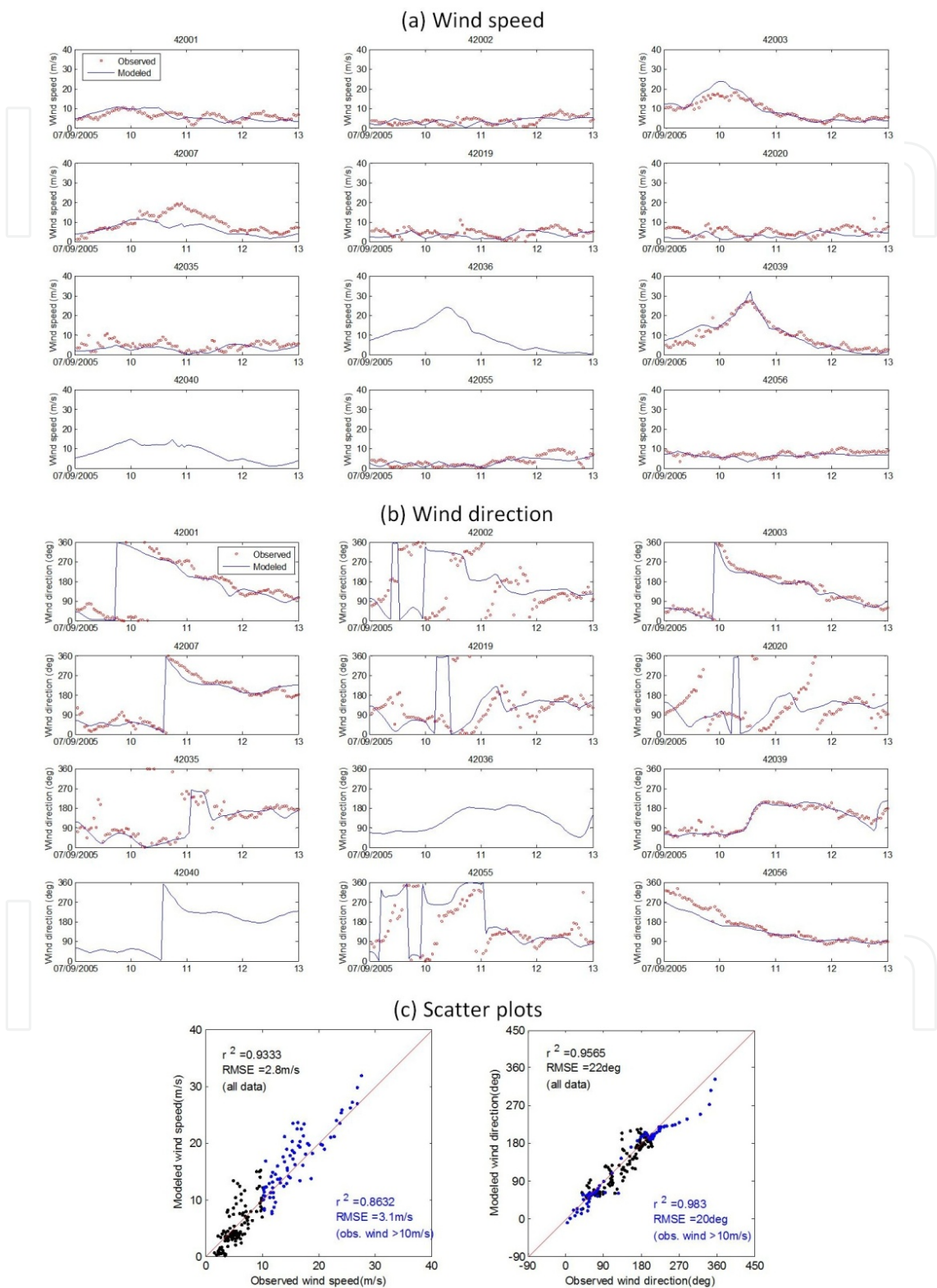

Figure 5. Wind comparisons at buoys in the Gulf of Mexico during Hurricane Dennis.
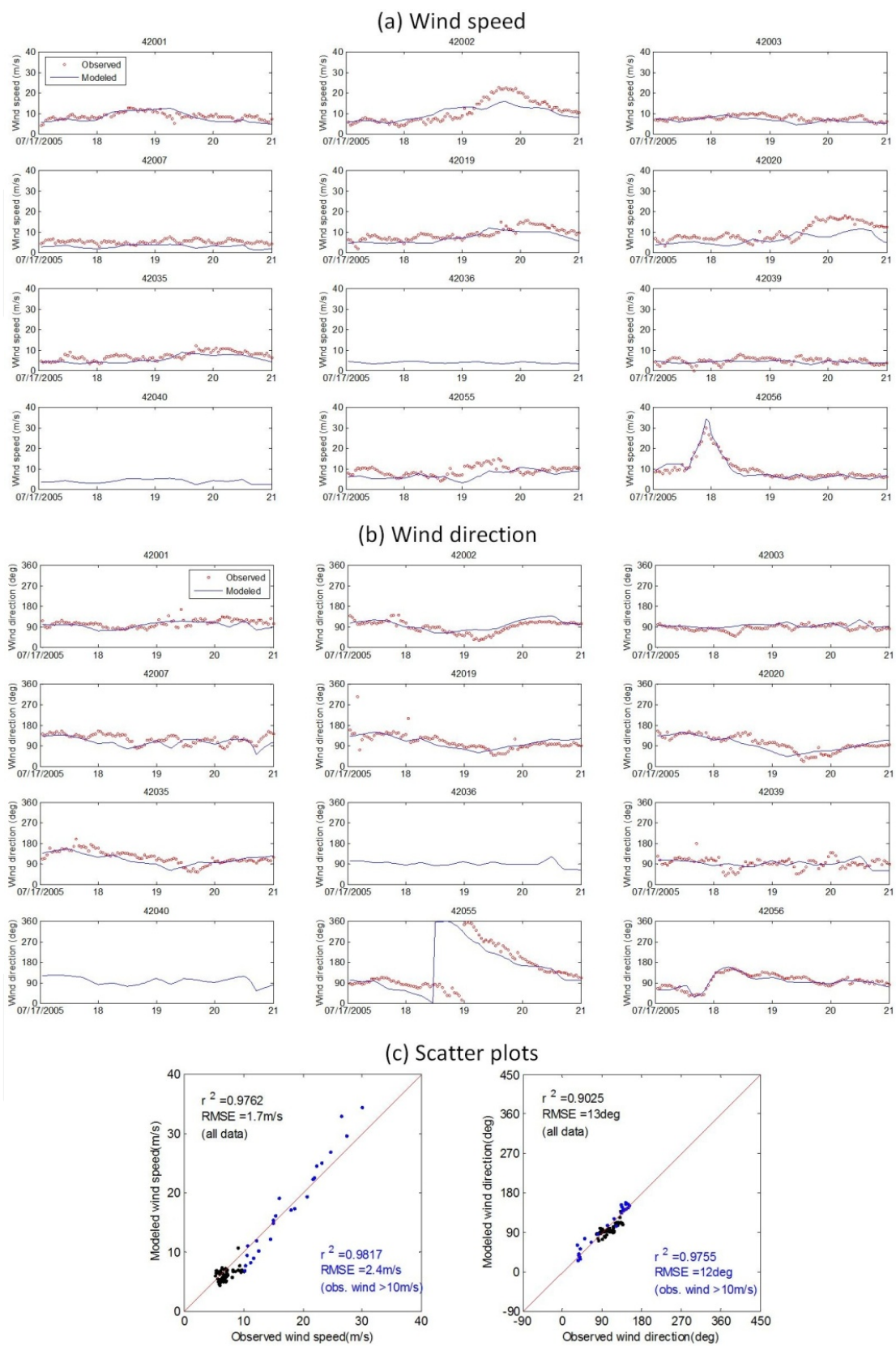
Figure 6. Wind comparisons at buoys in the Gulf of Mexico during Hurricane Emily.

Comparisons and scatter plots are shown in Figure 5. Wind speeds and wind directions at Buoy 42039 were very close to the hurricane track and our scheme validated reasonably well. There was some overestimation/underestimation of wind speed at Buoys 42003 and 42007, respectively. At other buoys where the background winds dominate, there were some errors mainly due to the operational model resolution. Buoys 42003 and 42039 were included in scatter plots. The overestimation of wind speed at Buoy 42003 increased the final RMSE to 3 ms^{-1}.

3.5. Hurricane Emily (2005)

Emily developed in the deep tropics, and by 13 July, had strengthened into a hurricane about 100 miles southeast of Grenada. Emily strengthen to a Category 5 hurricane late on 16 July at 17.1^{o}N 79.5^{o}W with maximum sustained surface wind speeds near 140 knots and a minimum surface pressure of 929 mb. Emily maintained hurricane intensity after crossing over into the southwestern Gulf of Mexico. Once back over open water, Emily again began intensifying, and approached extreme northeastern Mexico as a potent Category 3 hurricane with maximum sustained surface winds of 110 knots. Emily made landfall on July 20 around San Fernando, Mexico, and weakened to a tropical depression inland next day. Refer to NHC's report on Emily [25] for details.

Comparisons and scatter plots are shown in Figure 6. Similar with the situation in Dennis case, the modeled wind speeds and wind directions at Buoy 42056 which located close to the hurricane track agreed very well with the measurements. At Buoys 42002 and 42020, however, wind speeds are underestimated. Only Buoy 42056 was considered in scatter plots. The RMSE of wind directions is 12 degrees.

3.6. Hurricane Katrina (2005)

Katrina was an extraordinarily powerful and deadly hurricane that carved a wide swath of catastrophic damage and inflicted large loss of life. It was the costliest and one of the five deadliest hurricanes to ever strike the United States. Katrina started as a tropical depression on August 23, 2005, in the Atlantic Ocean. On August 28, Hurricane Katrina reached Category 5 status with wind speeds of 152 knots and a pressure of 902 mb near the center of the Gulf of Mexico. Hurricane Katrina made its second landfall between Grand Isle, Louisiana and the mouth of the Mississippi River on August 29, as a Category 3 hurricane with wind speeds of 110 knots and a low pressure of 920 mb. By 1500 UTC, Katrina made its third landfall near the Louisiana and Mississippi borderline as a Category 3 hurricane with wind speeds of nearly 105 knots. Refer to NHC's report on Katrina [26] for details.

Comparisons and scatter plots are shown in Figure 7. Buoys 42001, 42003, 42007 and 42030 were included in scatter plots. The modeled results were fairly good except for some overestimation of wind speed at Buoys 42036 and 42039. At Buoy 42040 where the winds are strongest among other buoys, the agreements of both wind speed and wind direction were excellent.
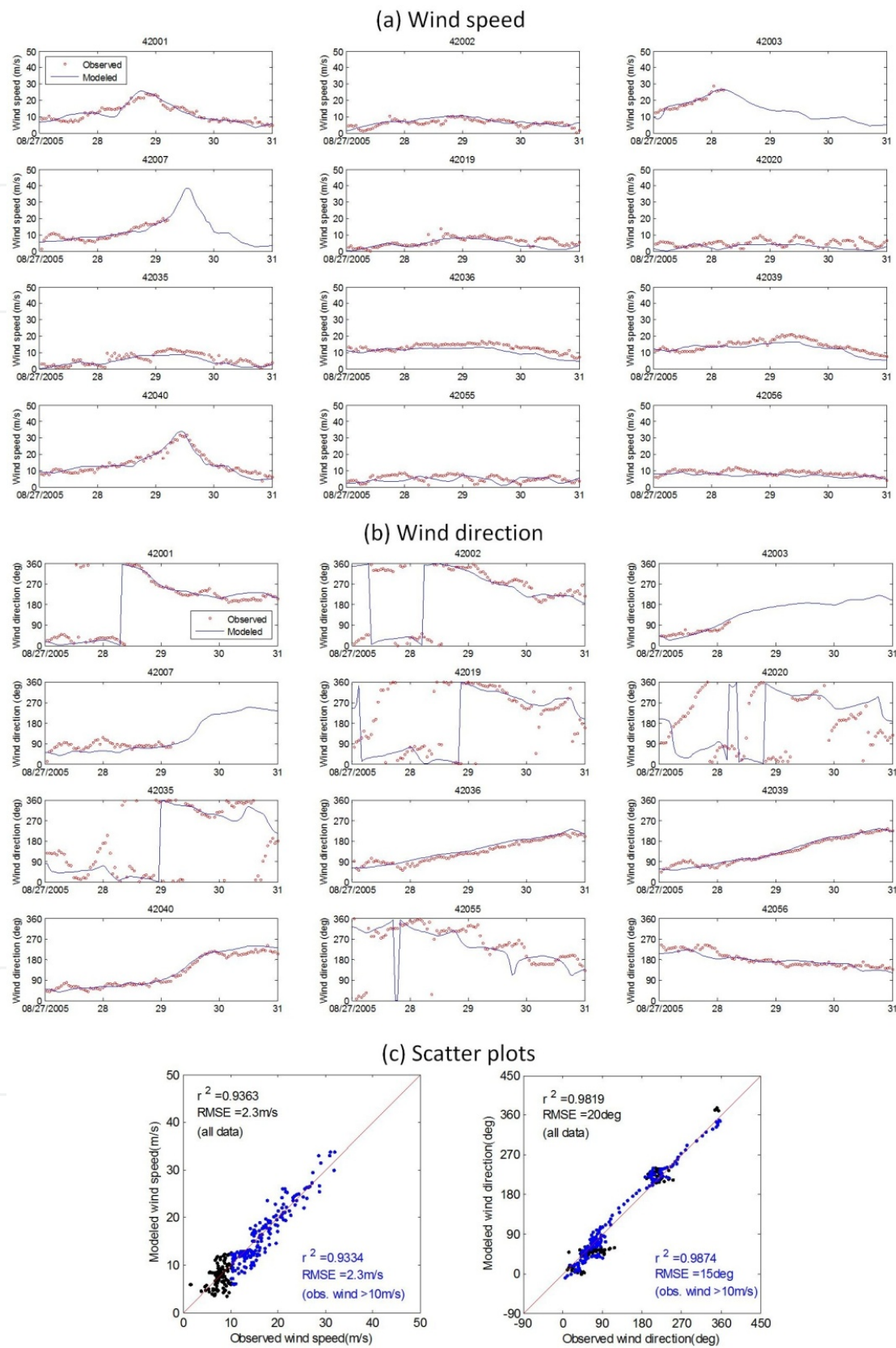
Figure 7. Wind comparisons at buoys in the Gulf of Mexico during Hurricane Katrina.

3.7. Hurricane Rita (2005)

Rita officially became a tropical storm on September 18, 2005, moved through the Florida Straits, and approached the Florida Keys on the 20th.
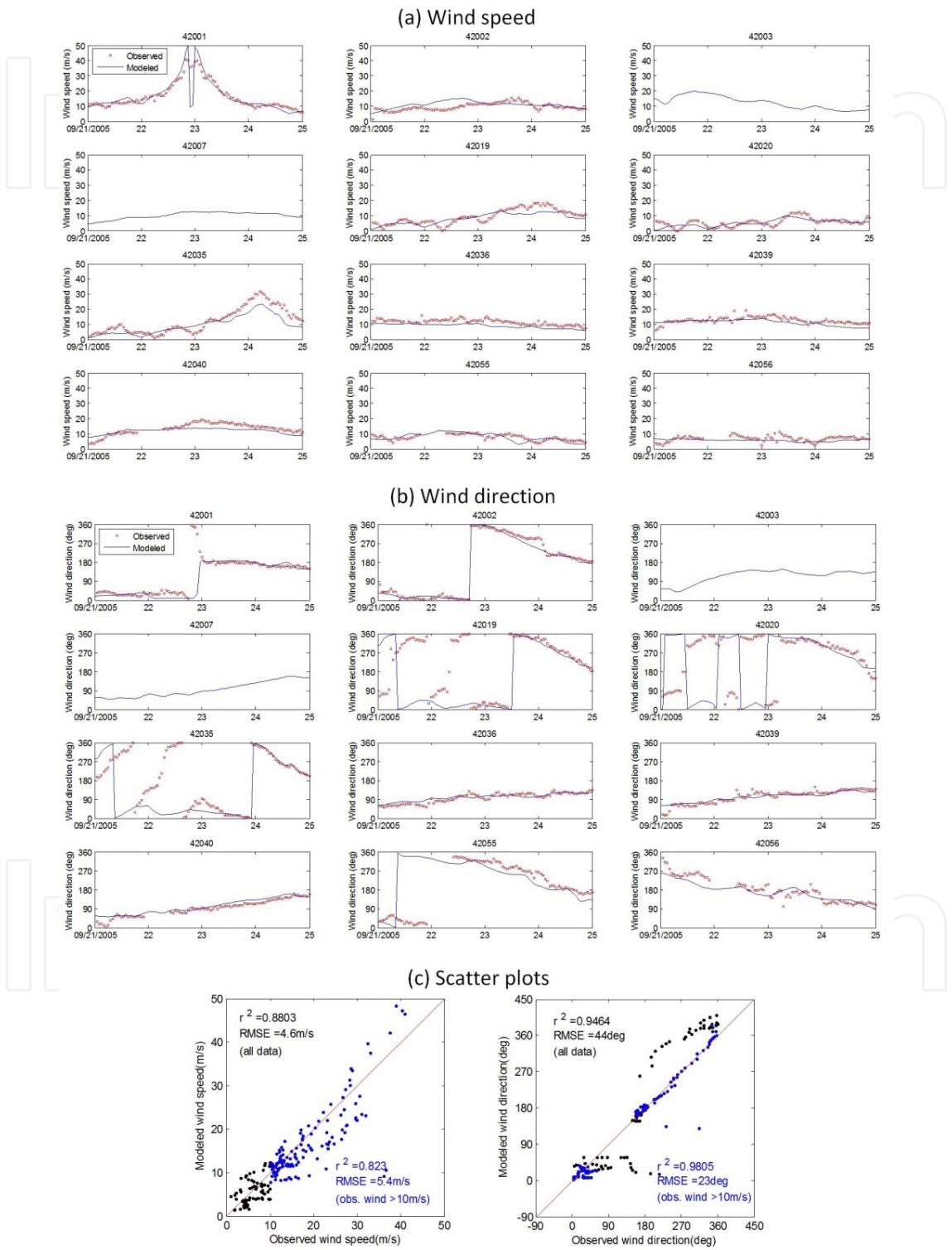

Figure 8. Wind comparisons at buoys in the Gulf of Mexico during Hurricane Rita.
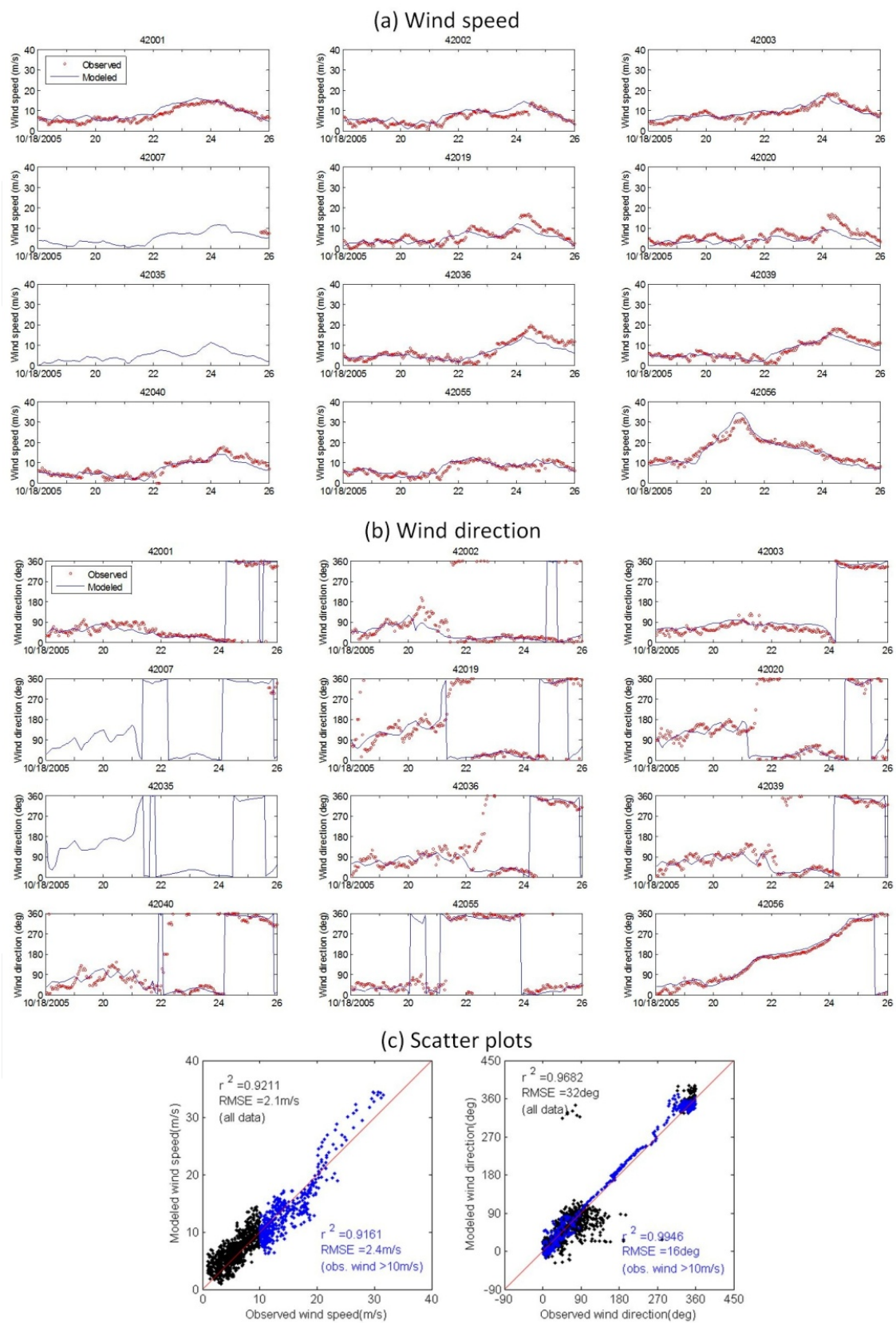
Figure 9. Wind comparisons at buoys in the Gulf of Mexico during Hurricane Wilma.

Rapidly intensifying, Rita tracked westward into the Gulf of Mexico and by the afternoon of the 21st, Rita had reached Category 5 strength, with winds of 143 knots. It peaked at 152 knots with a minimum central pressure of 897 mb. Weakening on the 22nd, Rita's intensity dipped and continued to weaken gradually over the next 36 hours prior to landfall. Rita tracked west-northwest during the 23rd and made landfall at the Texas/Louisiana border early on the 24th, at Category 3 strength with sustained winds of 104 knots. Refer to NHC's report on Rita [27] for details.

Comparisons and scatter plots are shown in Figure 8. Buoys 42001 and 42035 were included in scatter plots. Rita moved near Buoy 42001, and our scheme overestimated the peak wind speed a little bit. At Buoy 42035 before hurricane landfall, the model underestimated wind speeds, possibly due to a position error from the best track data. The scatter plots showed that the overall agreement was not very good in this case.

3.8. Hurricane Wilma (2005)

Hurricane Wilma formed in the second week of October 2005. From October 18, and through the following day, Wilma underwent explosive deepening over the open waters of the Caribbean; in a 30-hour period, the system's central atmospheric pressure dropped to the record-low value of 882 mb, while the winds increased to 161 knots. Hurricane Wilma then weakened to Category 4 status, and on October 21, it made landfall on Cozumel and on the Mexican mainland. Wilma reached the southern Gulf of Mexico before accelerating northeastward. The hurricane re-strengthened to hit Cape Romano, Florida, as a major hurricane. Wilma weakened as it quickly crossed the state, and entered the Atlantic Ocean. By October 26, it transitioned into an extratropical cyclone. Refer to NHC's report on Wilma [28] for details.

Comparisons and scatter plots are shown in Figure 9. At Buoy 52056, the hurricane winds were well reproduced. Agreements at other buoys were fairly accurate except for some underestimation of wind speed at a few buoys, e.g. 42036. Buoys 42001, 42002, 42003, 42036, 42039, 42055 and 42056 were included in scatter plots. It can be seen that the modeled wind directions agreed very well with the measurements for observed winds larger than 10 ms^{-1}.

3.9. Hurricane Gustav (2008)

Hurricane Gustav was a Category 4 hurricane and caused many deaths and considerable damage in Haiti, Cuba, and Louisiana. Gustav formed from a tropical wave that moved off the coast of Africa on August 13, 2008. Gustav strengthened into a hurricane before making landfall in Haiti. After significantly weakening over Haiti, Gustav encountered the warm waters of the northwestern Caribbean Sea, allowing for rapid intensification on August 30 before making landfall on the Isle of Youth, Cuba, and weakened to a tropical storm. Continuing into the Gulf of Mexico, Gustav regained some strength, making landfall near Cocodrie, LA as a Category 2 storm with maximum sustained winds of 90 knots. Refer to NHC's report on Gustav [29] for details.

Comparisons and scatter plots are shown in Figure 10. Buoys 42001, 42003, 42007, 42036, 42039 and 42040 were included in scatter plots. The modeled wind speeds matched the max-

imum wind speeds at each buoy reasonably well, although on September 2, the model over-estimated wind speeds. The agreement of wind direction was very good.
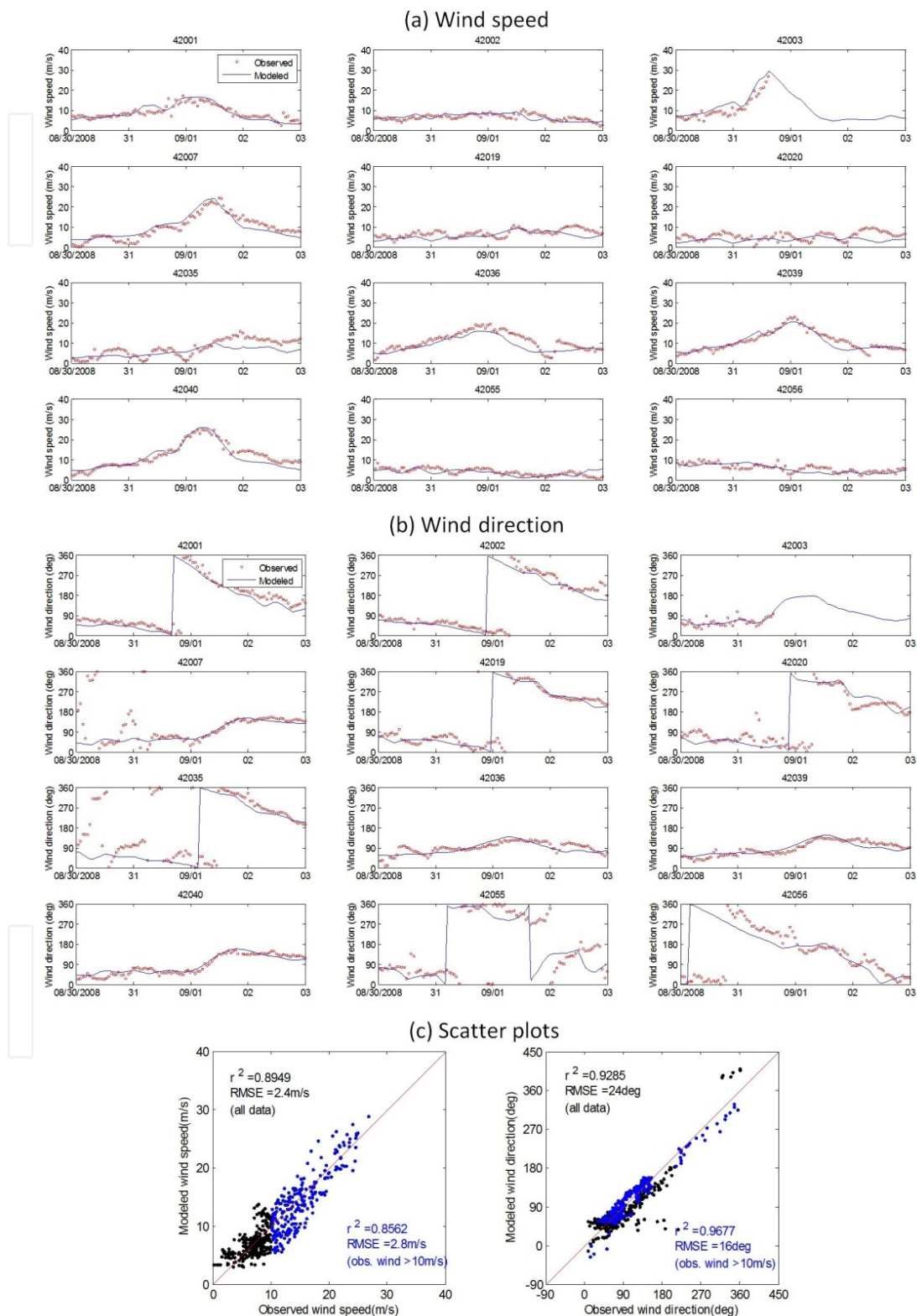

Figure 10. Wind comparisons at buoys in the Gulf of Mexico during Hurricane Gustav.

3.10. Hurricane Ike (2008)

Ike was a long-lived Cape Verde hurricane that caused extensive damage and many deaths across portions of the Caribbean and along the coasts of Texas and Louisiana.
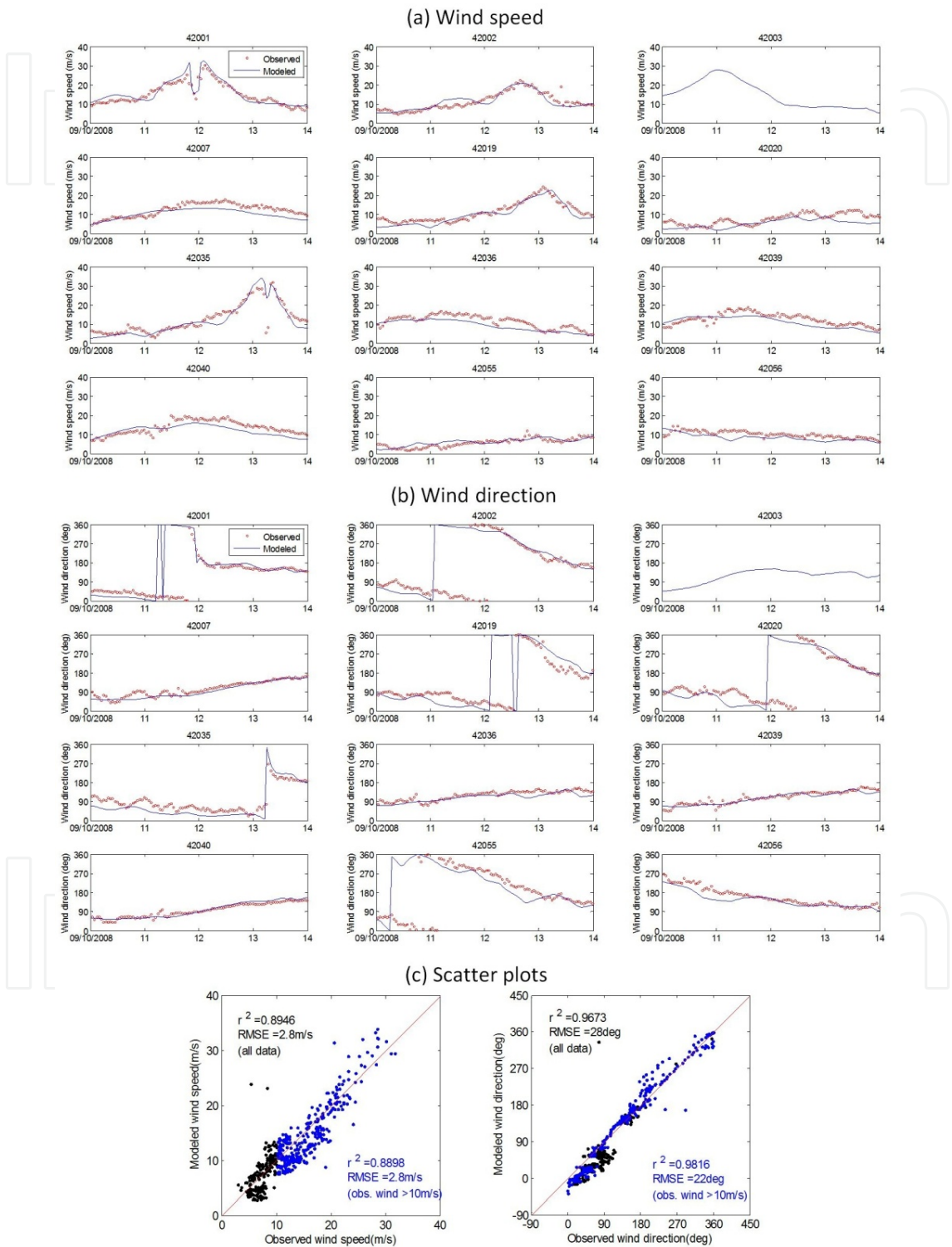

Figure 11. Wind comparisons at buoys in the Gulf of Mexico during Hurricane Ike.

Ike developed from a vigorous tropical wave that emerged off the west coast of Africa on August 29. Hurricane Ike made landfall across Great Inagua as a Category 4 hurricane on the morning of September 7, moving into the northeast Coast of Cuba as a Category 3 hurricane later that evening. Once Ike emerged into the Gulf of Mexico, the storm tracked more northwestward. Ike continued to grow on September 11. Ike continued tracking towards the upper Texas Coast, becoming better organized. Ike made landfall on Galveston Island September 13 as a strong Category 2 with sustained winds of 96 knots and a central pressure of 952 mb. Refer to NHC's report on Ike [30] for details.

Comparisons and scatter plots are shown in Figure 10. Buoys 42001, 42002, 42019, 42035 and 42040 were included in scatter plots. The wind evolution was reproduced quite well at Buoy 42001. The agreement at Buoy 42035 was also good although the calculated wind decrease was underestimated. Results at other buoys were reasonable except for some minor underestimation at Buoys 42036 and 42040 which were further away from Ike's center.

3.11. Summary

Scatter plots for eight hurricanes (except two 2002 hurricanes) at each related set of buoys are shown in Figure 12a. In addition, comparisons were made to another dataset which use the original shape parameter in Eq. (2) but restricted values between 1.0 and 2.5, used only the largest specified wind radii, and did not combine wind fields but did consider background operational model data, and is designated the "experimental wind model" (Figure 12b). The experimental model uses the highest available specified wind speed (34-, 50-, or 64-knot) and its 4-quadrant radii to generate the asymmetric hurricane wind, and the effect of the translational velocity is not excluded from those specified wind speeds. Scatter plots of observed winds versus experimental winds at same buoys for eight hurricanes are shown in Figure 12b. It can be seen that the overall RMSE of wind speeds was less than 3 ms^{-1} by using the improved parametric wind model. Without those improvements, the RMSE would increase to 3.4 ms^{-1} for observed winds larger than 10 ms^{-1}. The effect for wind directions was not as obvious as that for wind speed, but still was positive. Due to the low resolution of background winds, the RMSE of wind directions for all data was 30 degrees. When only considering larger winds (>10 ms^{-1}) which are mainly hurricane-dominated, the RMSE reduced to 19 degrees.

Among ten hurricane cases, the RMSE of modeled wind speeds for Hurricanes Isidore and Lili was relatively large, mainly due to the lack of radii information. Among the remaining eight cases, the RMSE in Rita case was larger than others. There are several factors which can cause model errors. The low resolution (uncertainty) of the location of hurricane track may induce significant changes in winds near hurricane center. Local weather processes which are not considered in the model would influence the results in some cases, especially for some nearshore buoys, e.g. 42007 and 42035. The error in best track data can ruin the results directly because the accuracy of a parametric wind model depends on the quality of the input hurricane parameters.
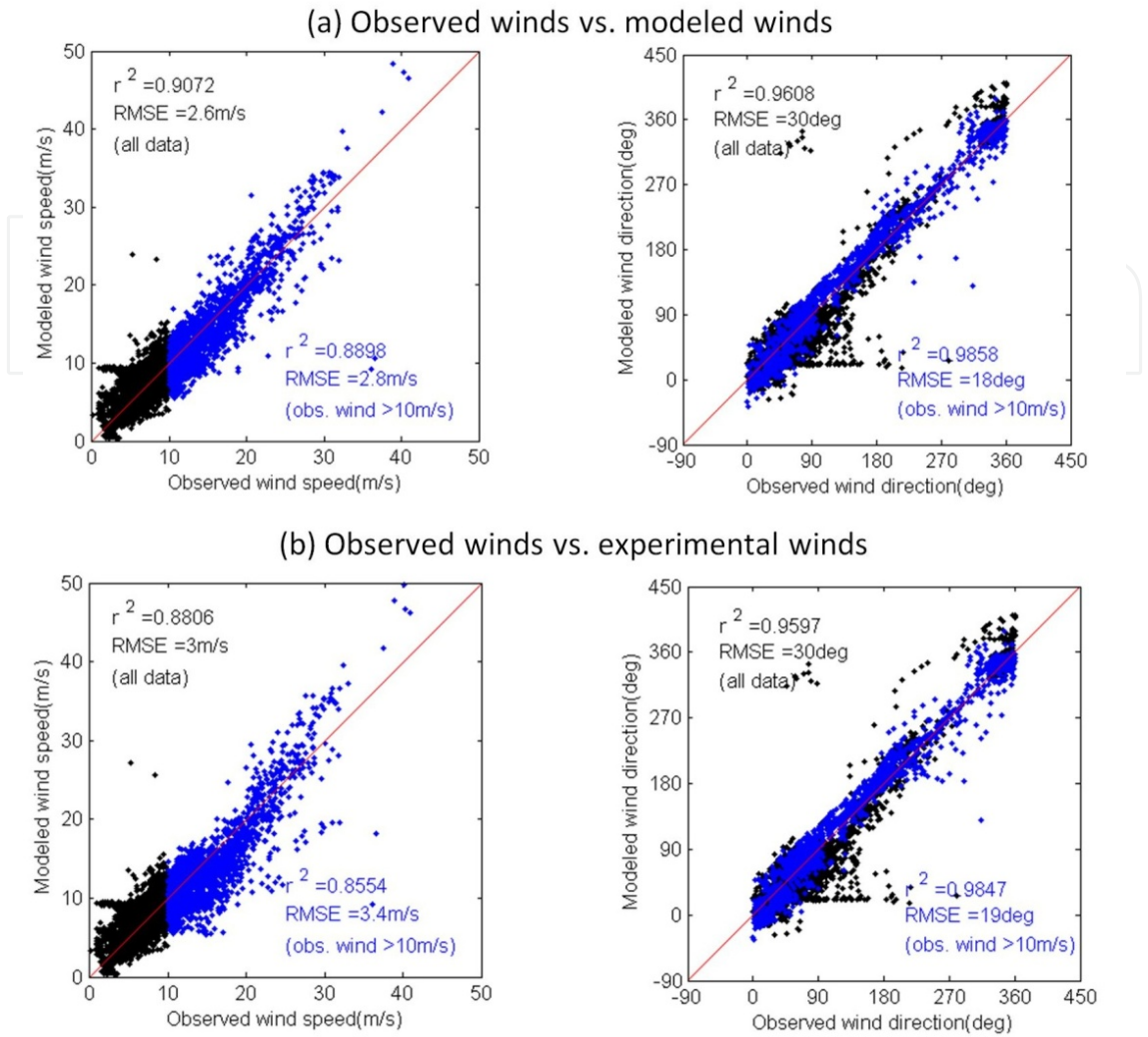
Figure 12. Scatter plots of observed winds versus (a) modeled winds and versus (b) experimental winds for eight hurricanes.

4. Discussion

4.1. Comparison with H*Wind

The H*Wind surface wind analysis [1] is considered to be one of the best hurricane wind estimates available. One question is whether this simple parametric model can reproduce the H*Wind distributions with the same data input? Two test cases for Hurricanes Katrina and Gustav were carried out. The difference from the previous cases is that input hurricane parameters were all taken from the H*Wind data except central pressure, which used best track. If applicable, the radii of all four-quadrant wind speeds (34, 50, 64 and 100 knots) were extracted from the H*Wind dataset and used in the wind model. Comparisons of wind field are shown in Figure 13. At 0000 UTC, August 29, 2005, during Katrina, the wind field produced by the wind

model agreed very well with the H*Wind distribution. The red circle is the extension of four points (four-quadrant radii) taken from the corresponding white circle in H*Wind. A good fitness between four red circles and four white circles in H*Wind means that the four-quadrant radii for four specified wind speeds can represent the actual wind structure in H*Wind. For Gustav at 0130 UTC, September 1, 2008, the red circles did not match the white ones well in H*Wind, which means a four-point scheme cannot capture asymmetric complexities. Otherwise, if the H*Wind asymmetry of wind structure is not very complicated, using 4-quadrant radii in this parametric wind model is capable of reproducing H*Wind distribution.
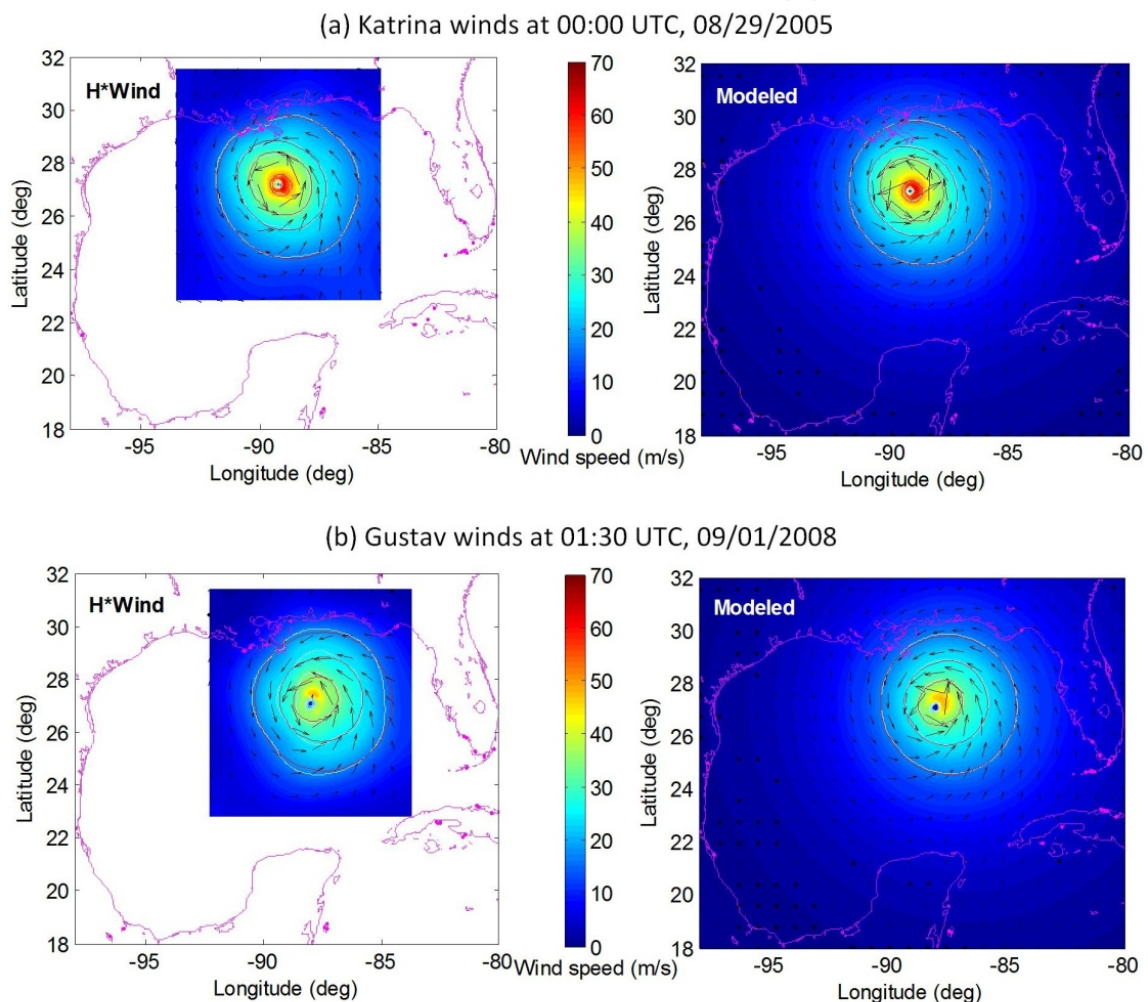

Figure 13. Comparisons of H*Wind distributions and modeled wind fields during (a) Hurricane Katrina and (b) Hurricane Gustav. Black arrows denote wind vectors. Write lines are the 34, 50, 64 and 100 knot (i.e., 17.5, 25.5, 33 and 51.5 ms⁻¹) wind speed contours. Red lines are the 34, 50, 64 and 100 knot wind speed contours fitted to the four input radii. Note that 100 knot contour is not applicable for Gustav.

Figure 14 depicts the comparison of the wind swaths generated from the H*Wind, the modeled winds and the experimental winds for Hurricanes Katrina and Gustav. In both cases, the modeled swath based on the improved parametric model agrees fairly well with the H*wind swath

of maximum winds, while the swath based on the experimental winds shows some obvious discrepancies. In experimental winds, the maximum wind band on the right side of the hurricane track appears to be "broader" than that in H*Wind or modeled winds, and on the left side, the experimental result seems "narrower". This means that without those improvements in the parametric wind model, the asymmetry in wind structure would be exaggerated.
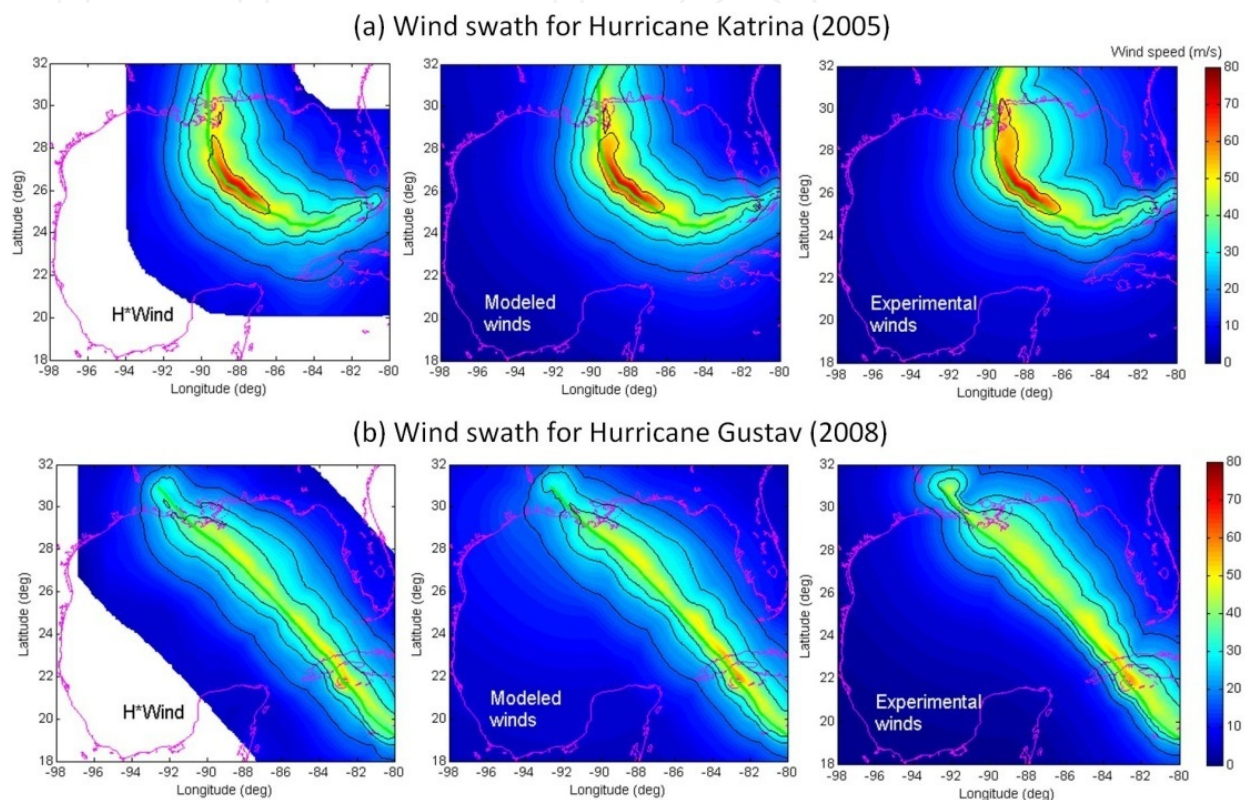

Figure 14. Wind swaths for H*Wind, modeled winds and experimental winds during (a) Hurricane Katrina and (b) Hurricane Gustav. Green line denotes hurricane track. Black lines are the 34, 50, 64 and 100 knot (i.e., 17.5, 25.5, 33 and 51.5 ms^{-1}) wind speed contours. Note that 100 knot contour is not applicable for Gustav.

4.2. Effects on surge and wave modeling

In order to further demonstrate the importance of those improvements in the parametric wind model, using Hurricane Gustav as an example, a fully coupled storm surge and wind wave modeling system [31] was employed to test the results. The ADCIRC model [32] and the SWAN model [33] are used to calculated storm surge and spectral waves, respectively. The same unstructured mesh from the Coastal Protection and Restoration Authority (CPRA) of Louisiana was adopted for both models. The CPRA mesh has about 1 million nodes and 2 million elements, covering the Gulf of Mexico and part of the Atlantic Ocean. The mesh resolution varies from 114 km in the Atlantic Ocean to about 20 m in Louisiana and Mississippi. Seven tidal constituents (M_2, S_2, N_2, K_1, O_1, K_2 and Q_1) are considered by harmonic constants at the open boundary in the Atlantic Ocean. The time steps are 1 hour and 1 sec-

ond for SWAN and ADCIRC, respectively. The non-stationary mode of SWAN in spherical coordinates is used. Thirty-one exponentially spaced frequencies from 0.0314 Hz to 0.5476 Hz with 36 evenly spaced directions (10° resolution) are utilized.
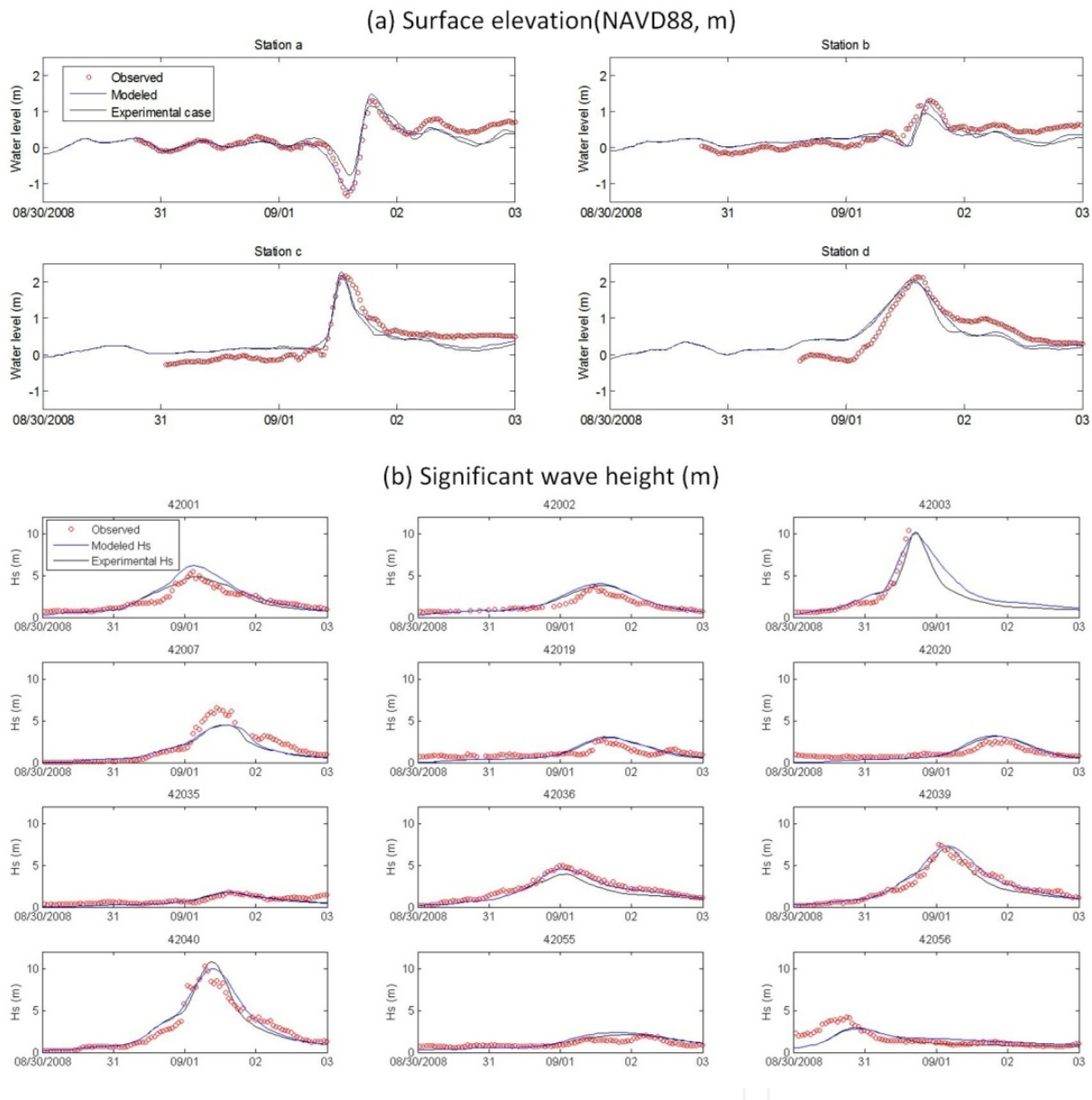

Figure 15. Comparisons of surface elevation and significant wave height using modeled winds with those using experimental winds during Hurricane Gustav.

Comparisons of modeled surge and waves with measurements are shown in Figure 15. Surge measurements were provided by some temporary gages deployed along Louisiana coast during the passage of Gustav [34]. The location of four gauges (Stations a-d) used in this paper are shown in Figure 1. Figure 15 shows an improvement of modeled results with measurements than the results driven by the experimental winds. At Station a, the modeled results reproduce the process of surge setup and set down as Gustav passed to

the right of the station. At Stations a and b, located at the left side of the track, the modeled maximum surge was larger than that by the experimental winds, while at Stations c and d, located on the right side of the track, the experimental case shows a surge higher than observed. Wave height comparisons showed that the modeled wave height agreed very well with the measurements, e.g. at Buoy 42036, except for some overestimation at Buoy 42001 and some underestimation at Buoy 42007. The experimental winds result in higher wave heights at Buoy 42040 located to the right side of the track, and lower wave heights at Buoy 42001 located to the left side. This is consistent with the swath results, narrower at the left side and broader at the right side.
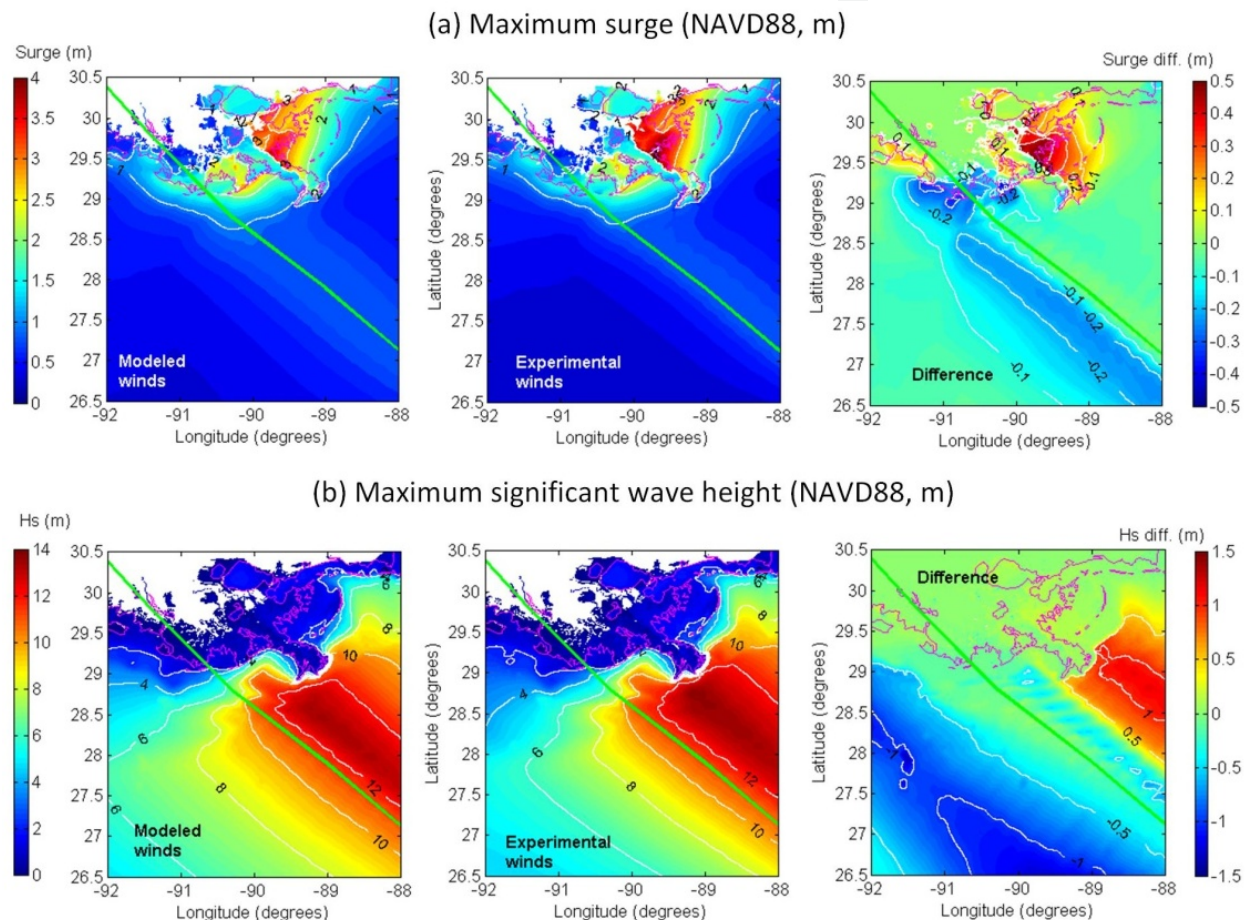

Figure 16. Comparisons of maximum surge and maximum significant wave height using modeled winds with those using experimental winds during Hurricane Gustav. Green line denotes hurricane track.

Distributions of maximum surge and maximum significant wave height driven by the modeled winds and by the experimental winds are compared in Figure 16. Difference distributions are provided as well to quantify the influence. During Gustav, counterclockwise winds pushed the water into the Chandeleur Sound and blocked by the east bank of the Mississippi River, which caused more than 3 m of storm surge. The maximum wave height was about 14 m off shore at the right side of the hurricane track. Due to the exaggeration of wind asym-

metry in the experimental winds, compared to the modelled wind results, the maximum surge at the right bank of the Mississippi River increased about 0.5 m, and the surge along the left side of the track decreased about 0.2 m. Simultaneously, the maximum wave height at the right side of the track increased up to 1.2 m, while at the left side decreased by more than 1 m. It is shown that the accuracy of hurricane winds is of great importance to the results of storm surge and waves. Without the improvements in the parametric wind model, the difference would be about 10% on both sides of the hurricane track.

5. Conclusions

Ten historical hurricanes were selected to test the performance of a revised parametric wind model. The revisions include: retention of the Coriolis effect in the shape parameter B; translational velocity excluded before applying the Holland-type vortex to avoid exaggeration of the wind asymmetry but added back in at the end of the procedure; and a weighted composite wind field that makes full use of all wind parameters, not just the largest available specified wind speed and its 4-quadrant radii. This scheme was validated against buoy and tide gauge observations. The overall RMSE for wind speed and wind direction is 2.8 ms^{-1} and 18 degrees for observed winds larger than 10 ms^{-1}. Without those improvements, the two values of RMSE increase to 3.4 ms^{-1} and 19 degrees for another dataset (designated the "experimental" dataset) which used the original shape parameter in Eq. (2) but restricted values between 1.0 and 2.5, used only the largest specified wind radii, and did not combine wind fields but did consider background operational model data.

The low resolution of hurricane locations, local weather processes, and error in best track data may affect the accuracy of the wind model. By comparing with H*Wind, it is found that the wind model has the capability to reproduce the H*Wind distribution if the asymmetry of wind structure is not too complicated. The wind swath results produced by the experimental winds showed that the asymmetry in wind structure was exaggerated. The importance of those improvements in the parametric wind model were further demonstrated through the effects on storm surge and hurricane wave modeling by using a fully coupled surge-wave model during Hurricane Gustav. The modeled results gave better agreements with observed surges and waves than the experimental results. Due to the exaggeration of wind asymmetry in experimental winds, the difference in storm surge and hurricane waves was about 10% on both sides of the hurricane track.

It should be noted that the number of parameters in the hurricane forecasts affects the accuracy of the parametric wind model. If more information — either the 4-quadrant radii of additional specified wind speeds (e.g., 100 knots) or more radii (e.g. at eight directions instead of only at 4 quadrants) for each specified wind speed — was available, the improved parametric model can deal with more complicated asymmetry in wind structure and produce more accurate wind fields for major hurricanes.

Acknowledgements

Author details

Kelin Hu[1], Qin Chen[2*] and Patrick Fitzpatrick[3]

*Address all correspondence to: qchen@lsu.edu

1 Department of Civil and Environmental Engineering, Louisiana State University, Baton Rouge, USA

2 Department of Civil and Environmental Engineering, and Center for Computation and Technology, Louisiana State University, Baton Rouge, USA

3 Geosystems Research Institute, Mississippi State University, Stennis Space Center, USA

References

[1] Powell, M. D., Houston, S. H., Amat, L. R., & Morisseau-Leroy, N. (1998). The HRD real-time hurricane wind analysis system. *Journal of Wind Engineering and Industrial Aerodynamics*, 77 & 78, 53-64.

[2] Thompson, E. F., & Cardone, V. J. (1996). Practical modeling of hurricane surface wind fields. *Journal of Waterway, Port, Coastal, and Ocean Engineering*, 122(4), 195-205.

[3] Vickery, P. J., Skerlj, P. F., Steckley, A. C., & Twisdale, L. A. (2000). Hurricane wind field model for use in hurricane simulations. *Journal of Structural Engineering*, 126, 1203-1221.

[4] Cox, A. T., Greenwood, J. A., Cardone, V. J., & Swail, V. R. (1995). An interactive objective kinematic analysis system. Banff, Alberta, Canada. *In: Proc Fourth Int Workshop on Wave Hindcasting and Forecasting*, Atmospheric Environment Service, 109-118.

[5] Vickery, P. J., & Skerlj, P. F. (2005). Hurricane gust factors revisited. *Journal of Structural Engineering*, 131, 825-832.

[6] Holland, G. J., Belanger, J. I., & Fritz, A. (2010). A revised model for radial profiles of hurricane winds. *Monthly Weather Review*, 138, 4393-4401.

[7] Vickery, P. J., & Twisdale, L. A. (1995). Wind-field and filling models for hurricane wind-speed predictions. *Journal of Structural Engineering*, 121, 1700-1709.

[8] Schloemer, R. W. (1954). Analysis and synthesis of hurricane wind patterns over Lake Okeechobee, *NOAA Hydrometeorology Report 31*, Department of Commerce and U.S. Army Corps of Engineers, U.S. Weather Bureau, Washington, D.C., 49.

[9] Leslie, L. M., & Holland, G. J. (1995). On the bogussing of tropical cyclones in numerical models: A comparison of vortex profiles. *Meteorology and Atmospheric Physics*, 56, 101-110.

[10] Jelesnianski, C. P. (1966). Numerical computations of storm surges without bottom stress. *Monthly Weather Review*, 94, 379-394.

[11] Holland, G. J. (1980). An analytic model of the wind and pressure profiles in hurricanes. *Monthly Weather Review*, 108, 1212-1218.

[12] Hu, K., Chen, Q., & Kimball, S. K. (2012). Consistency in hurricane surface wind forecasting: an improved parametric model. *Nature Hazards*, 61, 1029-1050.

[13] Willoughby, H. E., & Rahn, M. E. (2004). Parametric representation of the primary hurricane vortex. Part I: Observations and evaluation of the Holland (1980) model. *Monthly Weather Review*, 132, 3033-3048.

[14] Willoughby, H. E., Darling, R. W. R., & Rahn, M. E. (2006). Parametric representation of the primary Hurricane Vortex. Part II: A new family of sectionally continuous profiles. *Monthly Weather Review*, 134, 1112-1120.

[15] Holland, G. J. (2008). A revised hurricane pressure-wind model. *Monthly Weather Review*, 136, 3432-3445.

[16] Levinson, D. H., Vickery, P. J., & Resio, D. T. (2010). A review of the climatological characteristics of landfalling Gulf hurricanes for wind, wave, and surge hazard estimation. *Ocean Engineering*, 37, 13-25.

[17] Vickery, P. J., Masters, F. J., Powell, M. D., & Wadhera, D. (2009). Hurricane hazard modeling: The past, present, and future. *Journal of Wind Engineering and Industrial Aerodynamics*, 97, 392-405.

[18] Xie, L., Bao, S., Pietrafesa, L. J., Foley, K., & Fuentes, M. (2006). A real-time hurricane surface wind forecasting model: Formulation and verification. *Monthly Weather Review*, 134, 1355-1370.

[19] Mattocks, C., & Forbes, C. (2008). A real-time, event-triggered storm surge forecasting system for the state of North Carolina. *Ocean Modelling*, 25, 95-119.

[20] National Oceanic and Atmospheric Administration, National Weather Service, National Centers for Environmental Prediction, National Hurricane Center. *Automated Tropical Cyclone Forecast (ATCF) best track data*, ftp://ftp.tpc.ncep.noaa.gov/atcf/archive/.

[21] Avila, L. A. (2002). *Hurricane Isidore: 14-27 September 2002. Tropical Cyclone Report*, National Oceanic and Atmospheric Administration, National Weather Service, Tropical Prediction Center, Miami, Florida.

[22] Lawrence, M. B. (2002). *Hurricane Lili: 21 September-04 October 2002. Tropical Cyclone Report*, National Oceanic and Atmospheric Administration, National Weather Service, Tropical Prediction Center, Miami, Florida.

[23] Stewart, S. R. (2004). *Hurricane Ivan: 2-24 September 2004. Tropical Cyclone Report*, National Oceanic and Atmospheric Administration, National Weather Service, Tropical Prediction Center, Miami, Florida.

[24] Beven, J. (2005). *Hurricane Dennis: 4-13 July 2005. Tropical Cyclone Report*, National Oceanic and Atmospheric Administration, National Weather Service, Tropical Prediction Center, Miami, Florida.

[25] Franklin, J. L., & Brown, D. P. (2005). *Hurricane Emily: 11-21 July 2005. Tropical Cyclone Report*, National Oceanic and Atmospheric Administration, National Weather Service, Tropical Prediction Center, Miami, Florida.

[26] Knabb, R. D., Rhome, J. R., & Brown, D. P. (2005). *Hurricane Katrina: 23-30 August 2005. Tropical Cyclone Report*, National Oceanic and Atmospheric Administration, National Weather Service, Tropical Prediction Center, Miami, Florida.

[27] Knabb, R. D., Brown, D. P., & Rhome, J. R. (2006). *Hurricane Rita: 18-26 September 2005. Tropical Cyclone Report*, National Oceanic and Atmospheric Administration, National Weather Service, Tropical Prediction Center, Miami, Florida.

[28] Pasch, R. J., Blake, E. S., Cobb, H. D., III, & Roberts, D. P. (2006). *Hurricane Wilma: 15-25 October 2005. Tropical Cyclone Report*, National Oceanic and Atmospheric Administration, National Weather Service, Tropical Prediction Center, Miami, Florida.

[29] Beven, J. L., & Kimberlain, T. B. (2009). *Hurricane Gustav: 25 August-4 September 2008. Tropical Cyclone Report*, National Oceanic and Atmospheric Administration, National Weather Service, Tropical Prediction Center, Miami, Florida.

[30] Berg, R. (2009). *Hurricane Ike: 1-14 September 2008. Tropical Cyclone Report*, National Oceanic and Atmospheric Administration, National Weather Service, Tropical Prediction Center, Miami, Florida.

[31] Westerink, J. J., Luettich, R. A., Feyen, J. C., Atikinson, J. H., Dawson, C., Roberts, H. J., Powell, M. D., Dunion, J. P., Kubatko, E. J., & Pourtaheri, H. (2008). A basin- to channel- scale unstructured grid hurricane storm surge model applied to Southern Louisiana. *Monthly Weather Review*, 136, 833-864.

[32] Luettich, R. A., Westerink, J. J., & Scheffner, N. W. (1992). ADCIRC: An advanced three-dimensional circulation model for shelves, coasts and estuaries. *Report 1: Theory and Methodology of ADCIRC-2DDI & ADCIRC-3DL. Technical Report, DRP-92-6*, U.S. Army Corps of Engineers.

[33] Booij, N., Ris, R. C., & Holthuijsen, L. H. (1999). A third-generation wave model for coastal regions:1. Model description and validation. *Journal of Geophysical Research*, 104(C4), 7649-7666.

[34] Kennedy, A. B., Gravois, U., Zachry, B., Luettich, R., Whipple, T., Weaver, R., Reynolds-Fleming, J., Chen, Q. J., & Avissar, R. (2010). Rapidly installed temporary gauging for hurricane waves and surge, and application to Hurricane Gustav. *Continental Shelf Research*, 30(16), 1743-1752.